FLEXURAL STRENGTH OF CFRP BOX BEAMS WITH DIFFERENT LAMINATE STRUCTURES

Hiroki Sakuraba[1], Takashi Matsumoto[2], and Toshiro Hayashikawa[3]

[1]Graduate School of Engineering, Hokkaido University, Sapporo, Japan,
Tel: 81-11-706-6172, e-mail: sakuraba_h@eng.hokudai.ac.jp
[2]Faculty of Engineering, Hokkaido University, Sapporo, Japan,
Tel: 81-11-706-6171, e-mail: takashim@eng.hokudai.ac.jp
[3]Faculty of Engineering, Hokkaido University, Sapporo, Japan,
Tel: 81-11-706-6170, e-mail: toshiroh@eng.hokudai.ac.jp

Received Date: July 6, 2012

Abstract

This paper presents an experimental study on the flexural strength of CFRP box beams with two laminate structures: a cross-ply (CP) and a quasi-isotropic (QI). Three specimens were prepared for each laminate structure. The specimens were tested under four point bending, and the material tests of each laminate structure were conducted. The bending tests showed that QI exhibited higher flexural strength than CP and that they had different failure configurations. Also, flexural strength is calculated based on beam theory with Tsai-Wu criterion or maximum stress criterion to be compared with the experimental one. Moreover, in order to discuss a buckling behavior, buckling stress is calculated. It is shown that the calculated flexural strength based on Tsai-Wu criterion agrees well with the experimental one and that the buckling stress exhibits higher value than compressive stress at the flexural strength in the bending test.

Keywords: Box beam, CFRP, Flexural, Flexure strength, Laminate structure

Introduction

Development of durable structures is an important focus in terms of maintenance of civil infrastructures. Recently, fiber reinforced polymer (FRP) has been studied in civil engineering because of its superior properties such as lightness, high strength, and non-corrosive nature. For now, FRP is widely applied to repairs and strengthening for columns and beams. In addition to these applications, FRP is expected for beams in bridges so as to achieve a high durability. In Japan, development of beams consisting of FRP has been conducted in order to clarify their flexural behaviors, which are glass fiber reinforced polymer (GFRP) beams [1], carbon fiber reinforced polymer (CFRP) beams [2], hybrid beams consisting of GFRP and CFRP [3], [4], and so on. Those developments show the applicability of FRP beams.

Since FRP is fabricated as a laminate composite, the mechanical properties of FRP are determined by the way to stack and orient individual layers called lamina. The way to stack and orient laminas is called laminate structure. To fulfill a good performance such as high stiffness and flexural strength, a proper design method of laminate structure for beams is important. However, further investigations are required since the design method is not fully established yet.

This study deals with CFRP which has higher stiffness and strength than other FRPs. Although CFRP is relatively expensive, development of beams with a high durability and safety can be possible if its properties are utilized efficiently. The authors examined the flexural behavior of CFRP box beams with six different laminate structures [5]. It is found that the different laminate structures clearly affect the flexural behaviors: stiffness, flexural strength, and failure configuration.

However, the flexural strength was lowered since a premature damage occurred. The premature damage was a longitudinal cracking at the corners between upper flange and web near loading points, which was due to the out-of-plane shear stress induced by concentrated loading transfer [6]. To examine the flexural strength of CFRP box beams in the case without the premature damage, further investigations are needed.

This paper presents the flexural strength of CFRP box beams with two laminate structures. In order to examine the flexural strength, three specimens were prepared for each laminate structure. The specimens were tested under four point bending, and the material tests of each laminate structure were conducted. Based on the bending and material tests, the flexural strength is discussed.

Bending Test Program

Specimens for Bending Tests

Two laminate structures were employed to examine the effect of different laminate structures. Three specimens were prepared for each laminate structure. The specimens consisted of laminates fabricated from carbon fiber and epoxy resin, and their material properties are shown in Tables 1 and 2, respectively. The specimens had a square box cross section with 100mm height, 100mm width and 5mm thickness, and a length of 1000mm.

Figure 1 shows laminate coordinate system 1-2 and lamina coordinate system x-y. The directions of 1 and 2 correspond to the longitudinal and transverse directions of the beam shown in the next section, respectively. The rotation angle between direction 1 and x is defined as fiber orientation angle.

The two laminate structures are shown in Table 3. For example, $[0/90]_5/[90/0]_5$, the first left side number means the fiber orientation angle of the first layer. The subscript five indicates that five [0/90] groups are continuously stacked. The two laminate structures are symmetric about the mid-plane. Specimen No.1 is a cross-ply which means that laminas are orthogonally stacked. Specimen No.2 is a quasi-isotropic which means that in-plane elastic behavior is isotropic. No.1 and No.2 are named CP and QI, respectively. The three

Table 1. Properties of Carbon Fiber

Property	Value	Remarks
Tensile strength F_f (MPa)	4900	Nominal value
Elastic modulus E_f (GPa)	240	Nominal value
Poisson's ratio ν_f	0.20	Assumed value*
Shear modulus G_f (GPa)	100	$G_f = E_f/2(1+\nu_f)$

*D. Hull and T. W. Clyne 2003 [7].

Table 2. Properties of Epoxy Resin

Property	Value	Remarks
Elastic modulus E_m (GPa)	3.5	Assumed value*
Poisson's ratio ν_m	0.38	Assumed value*
Shear modulus G_m (GPa)	1.27	$G_m = E_m/2(1+\nu_m)$

*D. Hull and T. W. Clyne 2003 [7].

Table 3. Laminate Structures of Specimens for Bending Tests

No.	Name	Laminate structure
1	CP	$[0/90]_5/[90/0]_5$
2	QI	$[0/45/-45/90]_5/[90/-45/45/0]_5$

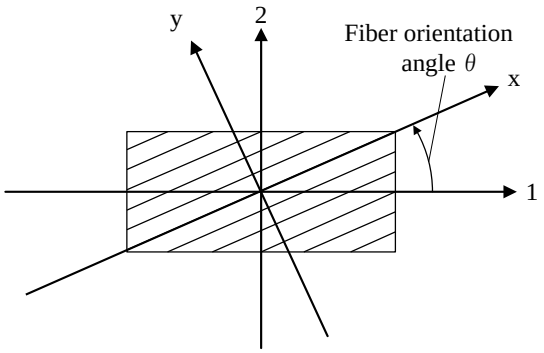

Figure 1. Laminate coordinate system 1-2 and lamina coordinate system x-y

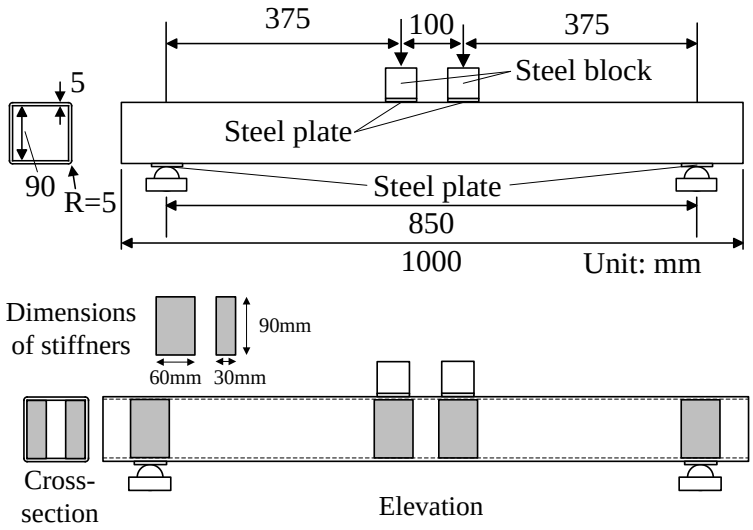

Figure 2. Loading condition and location of stiffeners

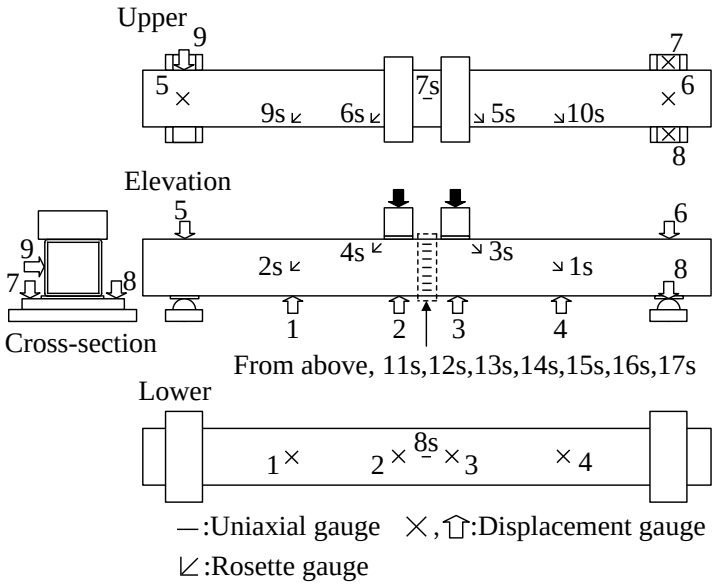

Figure 3. Location of instruments

Table 4. Properties of Stiffeners Made of Japanese Cedar

Property	Value	Remarks
Elastic modulus E (GPa)	7.5	Assumed values based on the reference [8]
Poisson's ratio ν	0.4	
Shear modulus G (GPa)	0.5	

Table 5. Laminate Structures of Specimens for Material Tests

No.	Name	Laminate structure
1	CP	$[0/90]_2/[90/0]_2$
2	QI	$[0/45/-45/90]_2/[90/-45/45/0]_2$

specimens of each laminate structure are distinguished by adding hyphen and number to the names, like CP-1 and QI-2.

Loading Condition and Configuration of Instruments

Loading condition and the location of stiffeners are shown in Figure 2. The specimens were tested under four point bending and under load control. The span, shear span, and flexural span were 850mm, 375mm, and 100mm, respectively. Stiffeners consisting of Japanese cedar were installed at the loading points and supports to prevent a premature damage that was observed in the past research [6]. Table 4 shows the properties of the stiffeners which were assumed based on nominal properties of Japanese cedar shown in the reference [8].

A preliminary test showed that the premature damage will not happen up to the flexural strengths of CP and QI if the stiffeners are installed. The premature damage was a longitudinal cracking at the corners between upper flange and web near loading points, which was due to the out-of-plane shear stress induced by concentrated loading transfer from loading plates [6]. Through the preliminary test, it was confirmed that the out-of-plane shear stress can be significantly reduced by installing the stiffeners.

Displacements and strains were measured at nine points and 17 points, respectively, as shown in Figure 3. White arrows show displacement gauges (No.1 to No.9), and black arrows show loading points. Rosette gauges and uniaxial gauges (No.1s to No.17s, the s after No. means strain gauges) are also illustrated in the figure.

Material Tests

Testing Method

The material tests of tension, compression, and shear of each laminate structure were conducted. In addition to the specimens for the bending tests, specimens of each laminate structure were fabricated for the material tests in order to apply Japanese Industrial Standards (JIS). Namely, the thickness of the laminates for the material tests was thinner (about 2mm) than those for the bending tests.

The laminate structures of each laminate structure for material tests are shown in Table 5. The material tests of tension, compression, and shear were conducted based on JIS K 7073, JIS K 7018, and JIS K 7079, respectively. The shapes of the specimens for the material tests are shown in Figure 4. Five specimens were prepared for each laminate structure. The material tests were run under displacement control at a loading rate of 1mm/min.

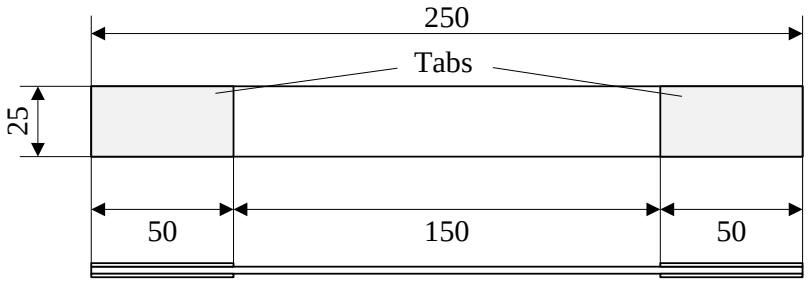

a) Shape for tensile and shear tests (Unit: mm)

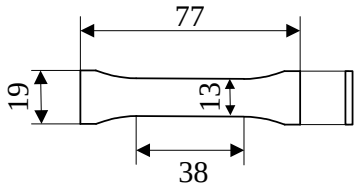

b) Shape for compressive tests (Unit: mm)

Figure 4. Shape of specimens for material tests

Table 6. Results of Material Tests

Property	CP		QI	
	Test*	**Theory**	**Test***	**Theory**
E_1 (GPa)	61.7	59.4	41.0	42.0
	(1.04)		(0.98)	
E_2 (GPa)	60.8	57.9	37.5	41.1
	(1.05)		(0.91)	
G_{12} (GPa)	4.20**	3.34	14.6	15.6
	(1.26)		(0.94)	
ν_{12}	0.050	0.045	0.31	0.33
	(1.11)		(0.94)	
ν_{21}	0.047	0.045	0.30	0.33
	(1.04)		(0.91)	
${\sigma_1}^T$ (MPa)	1006	-	645	-
${\sigma_1}^C$ (MPa)	352	-	272	-
${\tau_{12}}^U$ (MPa)	67.9**	-	252	-

*The values in ( ) are the ratio of the test values to the theoretical values. **Averaged values among four specimens due to a defect of one specimen.

Test Results and Discussions

The tendency of the material tests is discussed by comparing with the theoretical elastic constants of the specimens which are calculated based on classical lamination theory [9].

Results of the material tests and theoretical values are summarized in Table 6. The test values are the averaged ones among the five specimens except for G_{12} and ${\tau_{12}}^U$ of CP. In the case of CP, the test values are higher than the theoretical ones. On the other hand, in the case of QI, the test values are lower than the theoretical ones. Therefore, the different tendencies between them can be found. This can be answered by the shapes of the specimens. Namely, in the case of QI, the contribution of the diagonal (±45°) laminas to the stiffness of the laminates seems lowered when the laminates were shaped for the material tests as shown in Figure 4. According to this result, the strengths of QI seem also lowered.

Calculation Methods of Flexural Strength and Buckling Stress

Calculation methods of the flexural strength based on beam theory with Tsai-Wu criterion or maximum stress criterion are explained. In order to discuss a buckling behavior, a calculation method of buckling stress is also explained.

Flexural Strength Based on Tsai-Wu Criterion

Tsai-Wu criterion [10] consisting of components of longitudinal stress and in-plane shear stress is given as

$$F_1\sigma_1 + F_{11}\sigma_1^2 + F_{66}\tau_{12}^2 = 1 \tag{1}$$

$$\frac{F_1}{\sigma} = \frac{1}{\sigma_1^T} - \frac{1}{\sigma_1^C},\ F_{11} = \frac{1}{\sigma_1^T \cdot \sigma_1^C},\ F_{66} = \frac{1}{\left(\tau_{12}^U\right)^2} \tag{2}$$

where F_1, F_{11}, and F_{66} are Tsai-Wu's coefficients, σ_1 is the longitudinal normal stress, τ_{12} is the in-plane shear stress, ${\sigma_1}^T$ is the tensile strength in the longitudinal, ${\sigma_1}^C$ is the compressive strength in the longitudinal, and ${\tau_{12}}^U$ is the in-plane shear strength.

The flexural strength based on Tsai-Wu criterion can be obtained by substituting the longitudinal normal stress and in-plane shear stress based on beam theory into Equation (1) and is given by

$$P_{TW} = -\frac{\beta}{2\alpha^2} + \frac{1}{\alpha}\sqrt{1+\left(\frac{\beta}{2\alpha}\right)^2} \tag{3}$$

$$\alpha = \sqrt{F_{11}\left(\frac{xy}{2I}\right)^2 + F_{66}\left[\frac{1}{2I}\left\{\frac{h}{2}s - \left(\frac{y}{2} - \frac{h^2}{8}\right)\right\}\right]^2},\quad \beta = F_{11}\left(\frac{xy}{2I}\right) \tag{4}$$

where P_{TW} is the flexural strength based on Tsai-Wu criterion, x is the distance from the support (up to 375mm), y is the distance from the neutral axis, I is the second moment of area, s is the distance from the central point of the width of the flange, and h is the height of the beam.

Five calculation points of the flexural strength based on Tsai-Wu criterion are shown in Figure 5: a) corner of the upper flange at the loading point, b) corner of the lower flange at the loading point, c) center point of the web within the shear span, d) upper flange within the flexural span, and e) lower flange within the flexural span. Those points are indicated by X-Y-Z coordinate system as shown in Figure 5.

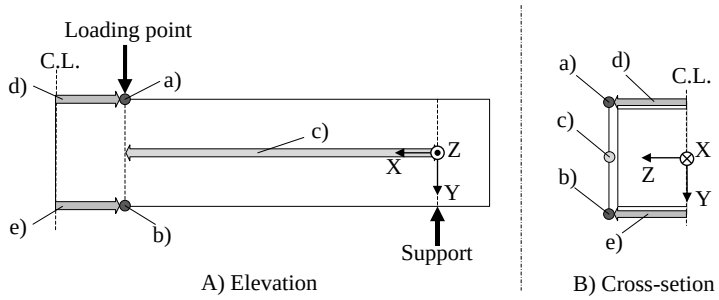

A) Elevation B) Cross-setion

a) Corner of upper flange at loading point , Coordinate (375, -50, 50)
b) Corner of lower flange at loading point , Coordinate (375, 50, 50)
c) Center point of web within shear span , Coordinate (0≦X≦375, 0, 50)
d) Upper flange within flexural span , Coordinate (375<X≦425, -50, 0≦Z≦50)
e) Lower flange within flexural span , Coordinate (375<X≦425, 50, 0≦Z≦50)

Figure 5. Calculation points of flexural strength

Flexural Strength Based on Maximum Stress Criterion

The flexural strength based on maximum stress criterion is determined when the longitudinal normal stress or in-plane shear stress reaches their strength and is given by Equation (5), Equation (6), and Equation (7).

$$P_C = -\frac{2I}{xy}\sigma_1^C \tag{5}$$

$$P_T = \frac{2I}{xy}\sigma_1^T \tag{6}$$

$$P_S = 2I\left\{\frac{h}{2}s - \left(\frac{y^2}{2} - \frac{h^2}{8}\right)\right\}^{-1}\tau_{12}^U \tag{7}$$

where P_C, P_T, and P_S are the flexural strength due to compression, tension, and shear failures, respectively.

Meanwhile, the flexural strength based on Tsai-Wu criterion corresponds to the flexural strength based on maximum stress criterion when only the longitudinal normal stress or in-plane shear stress is considered.

The flexural strength based on maximum stress criterion is calculated at a) corner of the upper flange at the loading point and b) corner of the lower flange at the loading point as shown in Figure 5 and is compared to the flexural strength based on Tsai-Wu criterion.

Buckling Stress

A calculation method of buckling stress based on the assumptions described below is explained. It is assumed that the upper flange within the flexural span is subjected to a uniform compressive force and is an orthotropic plate with simply supported edges.

The buckling stress of an orthotropic plate with simply supported edges [11] is given as

$$\sigma_{cr} = \frac{2\pi^2}{tb^2}\left\{\sqrt{D_{11}D_{22}} + D_{12} + 2D_{66}\right\} \tag{8}$$

$$D_{11} = \frac{E_1 t^3}{12\left(1-\nu_{12}\nu_{21}\right)}, \quad D_{22} = \frac{E_2}{E_1}D_{11}, \quad D_{12} = \nu_{12}D_{22}, \quad D_{66} = \frac{G_{12}t^3}{12} \tag{9}$$

where σ_{cr} is the bucking stress of an orthotropic plate with simply supported edges, t is the thickness of the laminates, b is the width of the upper flange, D_{11}, D_{22}, D_{12}, and D_{66} are the flexural rigidities of the laminates, E_1 is the elastic modulus in the longitudinal, E_2 is the elastic modulus in the transverse, ν_{12} is the Poisson's ratio, and G_{12} is the in-plane shear modulus.

Results and discussions

First, the failure configurations of each laminate structure are shown. Second, the flexural strengths of each laminate structure are discussed by comparing with calculated flexural strengths and buckling stresses.

Failure Configurations

Different failure configurations were observed between CP and QI. They failed near the steel plates at the loading points. The failure configurations of CP-2 and QI-3 are shown in Figures 6 and 7, respectively. Also, Figure 8 shows the failure locations of the six specimens and the outline of the failure configurations. The dashed lines mean a transverse cracking for CP and a ridge line due to a heaving for QI. The failure configurations of each laminate structure are almost the same although the failures occurred at the different sides of the steel plates as shown in Figure 8.

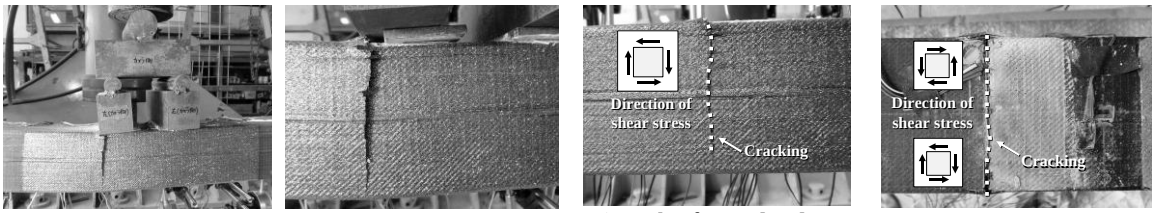

a) Around loading points b) Cracking in web c) Web after unloading d) Cracking in flange

Figure 6. Failure configuration in CP-2

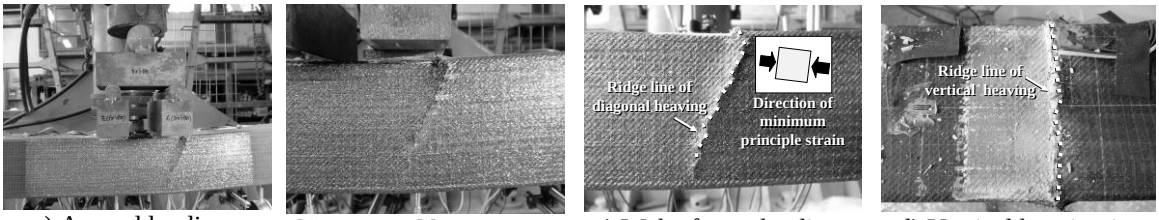

a) Around loading points b) Diagonal heaving in web c) Web after unloading d) Vertical heaving in flange

Figure 7. Failure configuration in QI-3

Figure 8. Failure locations and outline of failure configurations

In the case of CP-2, a transverse cracking was observed in web and upper flange. The cracking in the web developed toward the lower flange, and the cracking in the upper flange crossed transversely. This can be attributed to a relatively low shear strength as shown in Table 6. Namely, the cracking can occur along the direction of the in-plane shear stress shown in Figure 6 c) and d).

In the case of QI-3, unlike the transverse cracking in CP-2, a diagonal heaving in the web and a vertical heaving in the upper flange took place. This is presumably because QI has higher shear strength than CP as shown in Table 6. Namely, the diagonal heaving can be caused by the minimum principle strain which is oriented to the direction shown in Figure 7 c). The minimum principle strain of strain gauge No.4s was measured at the flexural strength of QI-3. The direction of the minimum principle strain shows a similar direction to the one which the ridge line of the heaving is oriented. The vertical heaving may occur in accordance with the direction of the loading which presses the upper flange.

Flexural Strength and Buckling Stress

QI exhibits higher flexural strength than CP, and calculated flexural strengths show that CP and QI fail when they satisfy Tsai-Wu criterion. Also, the buckling stresses of CP and QI exhibit higher values than the maximum longitudinal compressive stresses at their flexural strengths in the bending tests.

Figures 9 and 10 show load-displacement relationships at the loading point in CP and QI, respectively. The displacements are calculated by subtracting the averaged support-settlings between No.7 and No.8 from the averaged displacements between No.2 and No.3. As a result, averaged flexural strengths of CP and QI show 78.4kN and 96.0kN, respectively, and they failed as a brittle behavior.

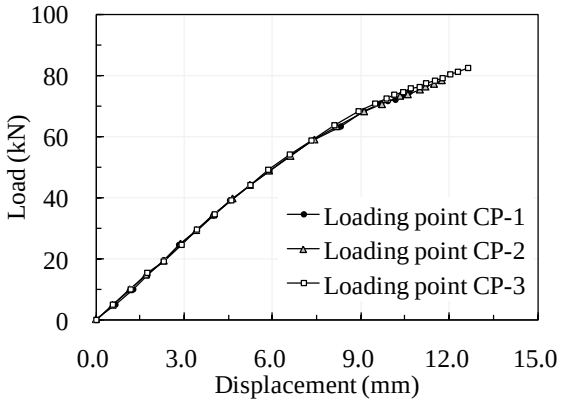

Figure 9. Load-displacement relationship in CP

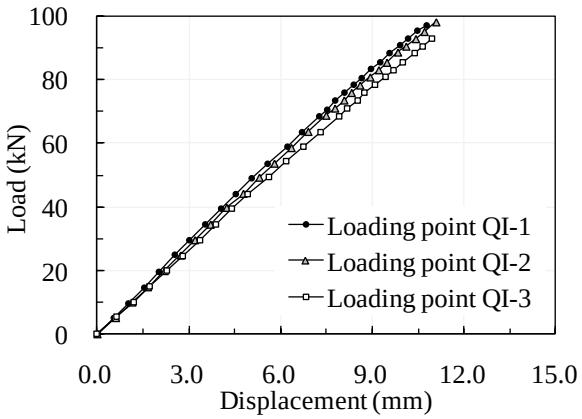

Figure 10. Load-displacement relationship in QI

Table 7. Comparison of Flexural Strengths

Description		Flexural Strength (kN)	
		CP	QI
Bending test	1	74.4	97.0
	2	78.5	98.2
	3	82.4	92.9
	Avg.	78.4	96.0
a) Corner of upper flange at loading point	P_{TW}	83.3	81.8
	P_C	108	83.0
	P_S	156	577
b) Corner of lower flange at loading point	P_{TW}	168	191
	P_T	307	197
	P_S	156	577
c) Center point of web within shear span	P_{TW} (=P_S)	104	385
d) Upper flange within flexural span	P_{TW} (=P_C)	108	83.0
e) Lower flange within flexural span	P_{TW} (=P_T)	307	197

Table 8. Comparison of Buckling and Compressive Stresses

Name	Buckling Stress (MPa)	Compressive Stress (MPa)
CP	304	256
QI	383	314

The flexural strength calculated by Equation (1) to Equation (7) is discussed. The comparison between the flexural strengths in the bending tests and the calculated ones is summarized in Table 7. Consequently, P_{TW} of CP and QI at a) corner of the upper flange at the loading point exhibit the smallest calculated flexural strengths, and the calculation point agrees with the failure location in the bending tests. Therefore, it is considered that CP and QI fail when they satisfy Tsai-Wu criterion.

In the case of CP, P_{TW} at a) corner of the upper flange at the loading point exhibits 83.3kN which is close to 78.4kN of the averaged flexural strength. On the other hand, P_C at a) corner of the upper flange at the loading point shows 108kN which higher than P_{TW} at the same calculation point as P_C. Therefore, it is thought that the in-plane shear stress significantly contributes to the failure.

In the case of QI, P_{TW} at a) corner of upper flange at the loading point shows 81.8kN which is clearly lower than 96.0kN of the averaged flexural strength. This can be answered by lower material strengths than actual ones. Namely, the material strengths of QI were weakly observed because of the shapes of the specimens as discussed in the section of Test results and discussion.

The buckling stress calculated by Equations (8) and (9) is discussed. The comparison between the buckling stress and the maximum longitudinal compressive stress in the bending tests at the flexural span and at the averaged flexural strength is summarized in Table 8. As a result, in both of CP and QI, the buckling stresses exhibit higher values than the maximum longitudinal compressive stresses. Although this result is based on the assumptions as described in the section of Buckling stress, it is concluded that CP and QI do not fail due to a buckling since P_{TW} of CP and QI at a) corner of the upper flange at the loading point agree relatively with the flexural strengths in the bending tests.

Conclusions

This paper presented the flexural strength and failure configuration of CFRP box beams with two laminate structures: a cross-ply and a quasi-isotropic. Four point bending tests and the material tests of each laminate structure were conducted. The conclusions are summarized as follows.

The bending tests showed that the specimens consisting of a quasi-isotropic exhibit clearly higher flexural strengths than those consisting of a cross-ply.

Results of calculated flexural strength and buckling stress showed the possibility that the specimens fail when they satisfy Tsai-Wu criterion and that a buckling at the upper flange within the flexural span does not occur before the failure caused by satisfying Tsai-Wu criterion in the bending tests.

Different failure configurations were observed in each laminate structure. A transverse cracking in the web and upper flange arose in the case of the specimens consisting of a cross-ply. A diagonal heaving in the web and a vertical heaving in the flange took place in the case of the specimens consisting of a quasi-isotropic.

Acknowledgements

This research was supported partially by the Kajima Foundation's Research Grant.

References

[1] S. Hino, B. Abdullah, R. Djamaluddin, K. Yamaguchi, K. Kawai, and K. Hayashi, "Behavior of GFRP pultruded I-600 beam under static and fatigue loadings," *Journal of Structural Engineering*, Vol. 51A, pp. 1267-1274, 2005.

[2] K. Sugiura, and Y. Kitane, "Static bending test of hybrid CFRP-concrete bridge superstructure," In: *Proceedings of US-Japan Workshop on Life Cycle Assessment of Sustainable Infrastructure Materials*, Hokkaido University, Japan, 2009.

[3] H. Mutsuyoshi, T. Aravinthan, S. Asamoto, and K. Suzukawa, "Development of new hybrid composite girders consisting of carbon and glass fibers," In: *Benefits of Composites in Civil Engineering*, COBRAE Conference 2007, University of Stuttgart, Germany, 2007.

[4] S. Asamoto, H. Mutsuyoshi, T. Aravinthan, and K. Suzukawa, "Experimental investigation of innovative hybrid composite girders with GFRP and CFRP," In: *The 4th International Structural Engineering and Construction Conference*, Taylor & Francis, London, United Kingdom, pp. 669-676, 2007.

[5] H. Sakuraba, T. Matsumoto, and T. Hayashikawa, "A study on the flexural behavior of CFRP box beams with different laminate structures," Paper presented at *the Twelfth East Asia-Pacific Conferences on Structural Enginnering and Construction*, EASEC12-38, pp.539-540, China, 2011.

[6] H. Sakuraba, T. Matsumoto, and T. Hayashikawa, "Flexural strength analysis of CFRP box beams with different laminate structures," In: *Proceedings of the Third Asia-Pacific Conference on FRP in Structures*, P03, Japan, 2012.

[7] D. Hull, and T.W. Clyne, Translated by H. Miyairi, K. Ikegami, and I. Kinabara, *An Introduction to Composite Materials,* 2nd Edition, Baihukan, 2003. (in Japanese)

[8] T. Chida, T. Sasaki, S. Usuki, H. Gotou, "Performance test and FEM analysis of a square steel tube-timber hybrid beam with a joint in the center," *Journal of Japan Society of Civil Engineers, Ser. A1 (Structural Engineering & Earthquake Engineering (SE/EE))*, Vol. 67, No. 1, pp. 108-120, 2011. (in Japanese)

[9] H. Sakuraba, T. Matsumoto, W. Horimoto, and T. Hayashikawa, "Influence of laminate structures on flexural behavior of CFRP box beams fabricated by VaRTM method," *Journal of Structural Engineering*, Vol. 58A, pp. 946-958, 2012. (in Japanese)

[10] M. Hyer, *Stress Analysis of Fiber-Reinforced Composite Materials*, WBC/ McGraw-Hill, 1997.

[11] L.P. Kollár, Local buckling of fiber reinforced plastic composite structural members with open and closed cross sections," *Journal of Structural Engineering*, Vol. 129, No. 11, pp. 1503-1513, 2013.